Acta Cryst. (1989). B45, 252–257

A Deformation Electron Density Study of Potassium Hydrogen Diformate

BY KERSTI HERMANSSON AND ROLAND TELLGREN

Institute of Chemistry, University of Uppsala, Box 531, *S*-751 21 *Uppsala, Sweden*

(*Received* 8 *August* 1988; *accepted* 3 *January* 1989)

Abstract

$KH(HCOO)_2$, $M_r = 130{\cdot}144$, orthorhombic, *Pbca*, $a = 17{\cdot}705\ (8)$, $b = 7{\cdot}349\ (4)$, $c = 7{\cdot}302\ (3)$ Å, $V = 950{\cdot}1\ (8)$ Å^3, $Z = 8$, $D_x = 1{\cdot}820\ (1)$ g cm^{-3}, λ(Mo $K\alpha$) $= 0{\cdot}71069$ Å, μ_x(calc.) $= 0{\cdot}973$ mm^{-1}, $F(000) = 528$, $T = 120$ K, $R(F^2) = 0{\cdot}033$ for 2109 unique reflexions. The deformation electron density in $KH(HCOO)_2$ has been studied by means of experimental X–N maps obtained at 120 K. The electron distributions in the two chemically similar but crystallographically non-equivalent formate groups are discussed and correlated with bond order. The density distribution in the short intermolecular O–H···O bond [2·437 (1) Å] is compared with experimental and theoretical maps in related compounds.

Introduction

The crystal structure of potassium hydrogen diformate was first determined by Larsson & Nahringbauer (1968) using single-crystal X-ray film data. Neutron diffraction studies have been carried out at room temperature at the Swedish R2 reactor and at 120 K at the high-flux reactor at the Institut Laue–Langevin (ILL) in Grenoble (Hermansson, Tellgren & Lehmann, 1983). A low-temperature X-ray dataset has been collected at 120 K and, together with the neutron data from ILL, forms the basis of the present X–N study. A theoretical electron density study has also been carried out in conjunction with this investigation (Taurian, Lunell & Tellgren, 1987).

The structure contains two chemically very similar but crystallographically nonequivalent formate groups, bonded together by a short hydrogen bond (O···O 2·45 Å). An electron density analysis of this compound allows the study of a number of subtle chemical features: the short hydrogen bond, the different carbon–oxygen bonds, and the similarities/differences between the two formate groups.

Experimental

Potassium hydrogen diformate, $KH(HCOO)_2$, was prepared from a mixture of formic acid and potassium hydroxide. Small cube-shaped crystals were recrystallized several times from an aqueous solution containing a small amount of formic acid. The crystal used for data collection had seven well-developed faces {100}, {032}, {023} and (010), and a calculated volume of $3{\cdot}73 \times 10^{-2}$ mm^3. It was mounted on an aluminium pin and coated with a thin protective layer by dipping it into a solution of polystyrene in chloroform. The data collection was carried out on a Stoe four-circle diffractometer using Mo $K\alpha$ radiation and a graphite monochromator. The cell parameters were refined from 15 high-angle reflexions in the 2θ range 22–47°. The diffractometer was modified to operate with an Air Products Displex CS-1003 refrigerator. The crystal was mounted on the cold finger and surrounded by a vacuum-tight beryllium cylinder. The absolute temperature was calibrated against the transition temperatures of KDP (123 K) and $KMnF_3$ (186·6 and 81·0 K). The temperature, 120 K, was stable to within ±0·5 K during data collection.

A total of 4503 integrated intensities was collected in a $\theta/2\theta$ scan mode and evaluated with the Lehmann–Larsen (1974) algorithm. This number includes symmetry-equivalent reflexions and reflexions measured more than once; these were measured as a monitor of systematic errors. For $\sin\theta/\lambda$ values above 0·85 Å^{-1} only those reflexions were measured which had an intensity greater than 2σ in a fast prescan. A 2% decrease in the test reflexions was treated according to McCandlish, Stout & Andrews (1975). The intensities were corrected for Lorentz, polarization and absorption effects, and averaged to 2322 independent reflexions with a consistency index $R_w = 0{\cdot}019$. Details of the data collection are given in Table 1.

Refinements

Conventional spherical-atom refinement

The quantity minimized in the full-matrix least-squares refinement was $\sum w(F_o^2 - F_c^2)^2$, where $w^{-1} = \sigma_c^2(F_o^2) + k^2F_o^4$, with σ_c^2 based on Poisson counting statistics and k set to 0·04. An anomalous-dispersion correction was included in the scattering factors. Reflexions with $I < 2\sigma(I)$ were considered unobserved and were not included in the refinement. An isotropic secondary-extinction parameter (Becker & Coppens, 1974) refined to an insignificantly low value. Thus, both the X-ray and neutron data sets used in this work were

0108-7681/89/030252-06$03.00

© 1989 International Union of Crystallography

Table 1. *Data collection and refinement*

	X-ray (120 K) (This study)	Neutron (120 K) (Hermansson *et al.*, 1983)
Diffractometer	Stoe, Uppsala	D9, ILL, Grenoble
Cooling device	Displex CS-1003	Displex CS-1003
Wavelength (Å)	0·71069	0·7228
Crystal volume (mm^3)	0·0373	47·4
Absorption (cm^{-1})	9·73	0·72
Transmission	0·738–0·769	0·815–0·825
Extinction	None	None
$(\sin\theta/\lambda)_{max}$ ($Å^{-1}$)	1·15	0·692
h, k, l range	0→34, 0→16, 0→16	0→24, 0→10, 0→10
No. of reflections measured	4503	1669
No. of reflections in refinement	2109	1095
No. of reference parameters	77	91
$R(F)$	0·023	0·025
$R(F^2)$	0·033	0·032
$R_w(F^2)$	0·071	0·047

Table 2. *Atomic positions in fractional coordinates* ($\times 10^5$)

Values for the conventional and high-order ($\sin\theta/\lambda > 0{\cdot}75$ $Å^{-1}$) refinements are given in the upper and middle rows, respectively. The neutron values from Hermansson *et al.* (1983) are given in the lower row. H atoms were fixed at their neutron values in the high-order refinement.

	x	y	z
K	46293 (1)	43953 (2)	28618 (2)
	46292 (2)	43954 (4)	28624 (4)
	46296 (5)	43978 (13)	28616 (14)
O(1)	15726 (4)	7255 (9)	7975 (10)
	15729 (7)	42768 (23)	57967 (21)
	15724 (4)	42723 (10)	57962 (10)
O(2)	5413 (4)	28361 (9)	48347 (8)
	5409 (8)	28354 (18)	48372 (21)
	5426 (3)	28371 (9)	48365 (10)
O(3)	29232 (4)	5229 (11)	1690 (10)
	29243 (8)	5271 (29)	1611 (24)
	29221 (4)	5253 (11)	1743 (11)
O(4)	40143 (3)	12508 (9)	14641 (9)
	40147 (7)	12499 (20)	14617 (22)
	40124 (3)	12504 (9)	14627 (10)
C(1)	12204 (4)	32031 (11)	47152 (10)
	12231 (8)	32019 (19)	47119 (20)
	12217 (3)	32020 (7)	47150 (8)
C(2)	33218 (5)	12473 (11)	14373 (11)
	33199 (8)	12525 (21)	14354 (21)
	33202 (3)	12488 (8)	14357 (8)
H(1)	15116 (82)	25983 (196)	37533 (216)
	15579 (0)	25820 (0)	36138 (0)
	15579 (7)	25820 (22)	36138 (22)
H(2)	30289 (79)	16031 (228)	24558 (203)
	30022 (0)	19063 (0)	25435 (0)
	30022 (8)	19063 (27)	25435 (24)
H(3)	23090 (115)	5828 (260)	4338 (268)
	22758 (0)	6320 (0)	4701 (0)
	22758 (7)	6320 (19)	4701 (19)

unaffected by extinction: an important prerequisite for a successful electron density study. In the final refinement, 77 parameters were varied: one scale factor, one extinction parameter, positional and anisotropic parameters for the non-H atoms, and positional and isotropic thermal parameters for the H atoms. A difference Fourier calculation of $F_{obs} - F_{calc}$ after the last cycle of refinement gave maximum and minimum residuals of 0·42 and −0·25 e $Å^{-3}$. The resulting R values and details of the refinement are given in Table 1.* The

*Lists of observed and calculated structure factors have been deposited with the British Library Document Supply Centre as Supplementary Publication No. SUP 51535 (22 pp.). Copies may be obtained through The Executive Secretary, International Union of Crystallography, 5 Abbey Square, Chester CH1 2HU, England.

Table 3. *Anisotropic thermal parameters* ($U_{ij} \times 10^4$ $Å^2$)

Values for the conventional and high-order ($\sin\theta/\lambda > 0{\cdot}75$ $Å^{-1}$) refinements are given in the upper and middle rows, respectively. The neutron values from Hermansson *et al.* (1983) are given in the lower row. H atoms were fixed at their neutron values in the high-order refinement. Isotropic thermal parameters were refined for the H atoms in the conventional X-ray refinement.

	U_{11}	U_{22}	U_{33}	U_{12}	U_{13}	U_{23}
K	132 (1)	135 (1)	141 (1)	9 (0)	−11 (0)	−11 (0)
	133 (1)	135 (1)	141 (2)	9 (1)	−10 (1)	−12 (1)
	124 (4)	127 (4)	131 (4)	11 (3)	−8 (4)	−7 (4)
O(1)	136 (3)	222 (3)	205 (3)	8 (2)	−21 (2)	60 (2)
	130 (3)	225 (5)	206 (4)	−20 (3)	−19 (3)	−67 (4)
	114 (2)	215 (3)	196 (3)	−10 (2)	−17 (2)	−61 (3)
O(2)	137 (2)	180 (2)	187 (3)	−26 (2)	−20 (2)	17 (2)
	130 (3)	186 (4)	190 (5)	−25 (3)	−17 (3)	10 (3)
	120 (2)	173 (3)	184 (3)	−24 (2)	−20 (2)	15 (3)
O(3)	138 (3)	328 (4)	253 (3)	23 (2)	−21 (2)	−111 (3)
	133 (4)	334 (7)	249 (5)	24 (5)	−24 (4)	−119 (5)
	125 (3)	315 (4)	253 (4)	23 (3)	−27 (3)	−113 (3)
O(4)	117 (2)	185 (3)	250 (3)	−3 (2)	−4 (2)	−12 (2)
	113 (3)	189 (4)	250 (5)	−6 (3)	−2 (3)	−11 (4)
	101 (3)	175 (3)	240 (3)	−2 (2)	−1 (2)	−21 (3)
C(1)	139 (3)	140 (3)	141 (3)	7 (2)	−8 (2)	5 (2)
	124 (4)	148 (4)	146 (4)	0 (3)	−9 (3)	−6 (3)
	116 (2)	131 (2)	133 (2)	2 (2)	−2 (2)	−2 (2)
C(2)	134 (3)	158 (3)	162 (3)	10 (2)	13 (2)	−2 (2)
	118 (4)	174 (4)	168 (5)	11 (3)	9 (3)	−13 (4)
	104 (2)	165 (2)	151 (3)	9 (2)	8 (2)	−9 (2)
H(1)	47 (36)					
	289 (0)	501 (0)	370 (0)	−29 (0)	91 (0)	−204 (0)
	289 (6)	501 (8)	370 (8)	−29 (6)	91 (6)	−204 (7)
H(2)	81 (42)					
	265 (0)	818 (0)	406 (0)	63 (0)	46 (0)	−309 (0)
	265 (6)	818 (12)	406 (8)	63 (7)	46 (6)	−309 (9)
H(3)	324 (60)					
	288 (0)	316 (0)	317 (0)	4 (0)	−43 (0)	−11 (0)
	288 (5)	316 (6)	317 (7)	4 (5)	−43 (5)	−11 (6)

scattering factors were taken from *International Tables for X-ray Crystallography* (1974); the computer programs used were from Lundgren (1982).

The final positional and thermal parameters are given in Tables 2 and 3. The neutron-derived quantities (Hermansson *et al.*, 1983) are supplied for comparison. Interatomic distances from the neutron study are given in Fig. 1.

High-order refinements

Refinements were performed with data cut-offs at $\sin\theta/\lambda = 0{\cdot}65$, 0·75 and 0·85 $Å^{-1}$, leaving 1105, 599 and 196 reflections, respectively. Positional and thermal parameters resulting from the 0·75 $Å^{-1}$ refinement are listed in Tables 2 and 3. The positions and thermal parameters for the H atoms were fixed at their neutron values. The *atomic positions* derived from the complete X-ray dataset generally agree within two combined standard deviations with the neutron-derived positions. The largest shifts, 0·005 (2) and 0·004 (2) Å, occur for O(3) and O(4), respectively. After the high-order refinement with $\sin\theta/\lambda \geq 0{\cdot}75$ $Å^{-1}$, the differences were 0·010 (3) Å for O(3) and 0·004 (3) Å for O(4).

Thermal parameters resulting from the full-data and the high-angle ($\sin\theta/\lambda \geq 0{\cdot}75$ $Å^{-1}$) X-ray refinements agree but are, on average, a factor 1·08 larger than the neutron-determined parameters. This discrepancy is anisotropic: U_{11} is the largest component for all atoms.

The $\langle U_{ii}(\mathrm{XD})/U_{ii}(\mathrm{ND})\rangle$ ratios are 1·16, 1·04 and 1·04 for $i = 1$, 2 and 3, respectively.

An alternative high-order refinement was carried out in which all positional parameters were fixed at their neutron-determined values; only the scale factor and thermal parameters were refined. This procedure resulted in thermal parameters very similar to those from the normal high-order refinement.

Deformation density maps

The *X–N* deformation density maps presented in this paper show the total electron density minus the superposition of spherical (or spherically averaged) atomic densities for H, C, O and K^+, calculated with positional and thermal parameters as derived from the neutron diffraction study (Hermansson *et al.*, 1983). The scale factor was determined (to 0·5039) in a separate refinement cycle; an increase of 3% from the conventional X-ray refinement value. The expected errors were estimated to be 0·05 e $Å^{-3}$ by comparison of chemically equivalent regions in the maps.

Results and discussion

The formate groups

A stereographic illustration of the unit cell of $KH(HCOO)_2$ was presented by Hermansson *et al.* (1983). Fig. 1 shows the structure of the $H(HCOO)_2^-$ ion and its nearest neighbours. The *X–N* density in the planes of the two formate groups is shown in Figs. 2(*a*) and 2(*b*). [The maps were presented in Taurian *et al.* (1987) to show the close resemblance with those obtained from an *ab-initio* calculation.]

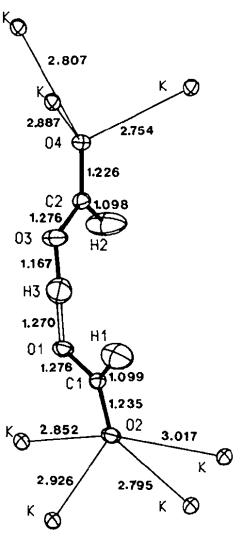

Fig. 1. The structure of the $H(HCOO)_2^-$ ion and its environment with bond distances (Å). By courtesy of *J. Chem. Phys.*

The general similarity between the two maps in Figs. 2(*a*) and 2(*b*) is apparent, and serves as an indicator of the quality of the neutron and X-ray data. The peak maxima in the C(1)–O(1) and C(1)–O(2) bonds are both ~0·45 e $Å^{-3}$, while the C(2)–O(3) and C(2)–O(4) maxima are 0·40 and 0·50 e $Å^{-3}$, respectively. Thus, within experimental accuracy, the carbon–oxygen bond densities in the two formate groups are identical. This correlates with the fact that the respective carbon–oxygen distances in the two formate ions are closely similar. The slight geometrical differences which do exist originate from differences in the K^+ environment [see Fig. 1 and the discussion of Hermansson *et al.* (1983)]. This feature is also responsible for the asymmetry in the hydrogen bond, as discussed by Taurian *et al.* (1987).

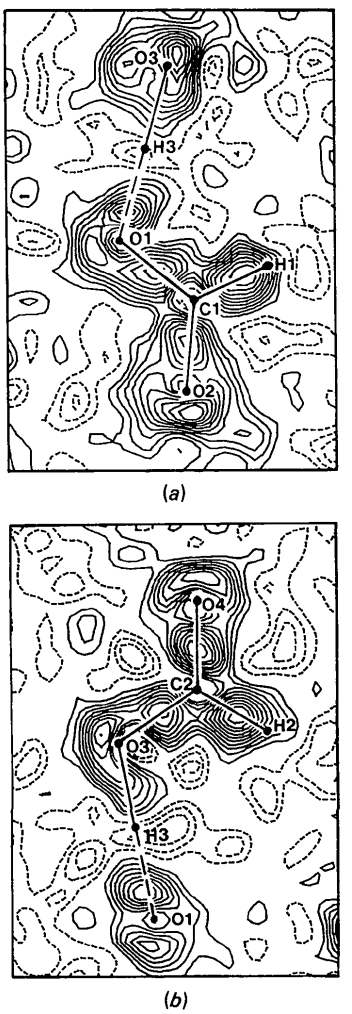

Fig. 2. (*a*), (*b*) *X–N* maps through the two formate groups. Electron excess is indicated by solid lines, deficiency by dashed lines; the zero contour is omitted. Contour interval: ±0·05 e $Å^{-3}$. By courtesy of *J. Chem. Phys.*

Judging from their bond lengths, the C(1)—O(1) and C(2)—O(3) bonds are expected to be of a type intermediate between a C—O and a C···O bond, while the other two lie between a C···O and a C=O bond. The density maps indicate a slightly higher bond order for the C(1)—O(2) and C(2)—O(4) bonds compared with the C(1)—O(1) and C(2)—O(3) bonds but, again, this effect is at the limit of experimental accuracy. Dynamic experimental deformation maps published for certain other compounds have revealed clearer differences between single and double C—O bonds. In $NaHC_2O_4.H_2O$ (Delaplane, Tellgren & Olovsson, 1989), for example, the peak maxima in the C—O, C···O and C=O bonds at 120 K were 0·30, 0·40 and 0·45 e Å^{-3}, respectively. In α-$(COOH)_2.2H_2O$ (Stevens & Coppens, 1980; Dam, Harkema & Feil, 1983), the dynamic peak maxima at 100 K were 0·40 e Å^{-3} in the C—O bond and 0·50 e Å^{-3} in the C=O bond. The corresponding peaks in the static deformation maps were 0·60 and 0·85 e Å^{-3}. A number of structures containing the $HCOO^-$ ion have been the subject of electron density analysis [NaHCOO, 120 K (Fuess, Bats, Dannöhl, Meyer & Schweig, 1982); $LiHCOO.H_2O$, room temperature (Thomas, Tellgren & Almlöf, 1975; Thomas, 1978; Harkema, de With & Keute, 1977); $Mg(HCOO)_2.2H_2O$, 100 K (van der Meulen & Feil, 1987); and α-$Ca(HCOO)_2$, 100 K (Fuess, Burger & Bats, 1981)]. In NaHCOO and $Mg(HCOO)_2.2H_2O$, the dynamic deformation maxima in the C···O bonds lie between 0·40 and 0·60 e Å^{-3}, while the room-temperature studies show peak heights of 0·25–0·30 e Å^{-3}.

Theoretical electron density maps obtained from quantum-mechanical calculations within the Hartree–Fock approximation display the character of the carbon—oxygen bond more clearly, since bonding effects are not smeared by vibrational motion, nor are the maps affected by random experimental error. Needless to say, the theoretical maps are affected by their own set of systematic errors, the most serious of which are normally an improper description of the crystalline environment, and an inadequate basis set. Several theoretical calculations for the α-$(COOH)_2.2H_2O$ system have been performed: LCAO–MO–SCF calculations on the oxalic acid molecule without (Johansen, 1979; Stevens, 1980) and with (Johansen, 1979) the short oxalic acid···water hydrogen bond, and local density functional calculations including the hydrogen-bond and crystal-field effects (Krijn, Graafsma & Feil, 1988). All calculations essentially agree in giving a static deformation density of approximately 0·55 e Å^{-3} in the C—O bond and 0·75 e Å^{-3} in the C=O bond. For $NaHC_2O_4.H_2O$ (Lunell, 1984), the C—O, C···O and C=O bonds showed peak maxima of 0·6, 0·7 and 0·8 e Å^{-3}, respectively. Calculations on the present compound by Taurian *et al.* (1987) gave C(1)—O(1) and C(2)—O(3) bond peak maxima of 0·7 e Å^{-3}, and C(1)—O(2) and C(2)—O(4) maxima of 0·8 e Å^{-3}. The theoretical and experimental results are thus in good agreement in terms of the relative peak heights. The vibrational motion reduces the peak densities by ~ 50%.

Oxygen lone-pair regions

The nonbonding regions ('lone-pair' regions) around the four O atoms clearly represent quite different bonding situations (*cf.* Figs. 2*a* and 2*b*). The O(2) and O(4) atoms are expected to be close to sp^2-hybridized. The experimental maps show elongated density lobes in the molecular plane; though not completely resolved, they are nonetheless in good agreement with the theoretical maps, considering the effects of thermal smearing. The situation is different for the O(1) and O(3) atoms which participate in the short hydrogen bond. As discussed previously (Hermansson *et al.*, 1983; Taurian *et al.*, 1987), the H(3) atom can be considered as shared between the two O atoms. This means that the hybridization is of neither sp^3- nor sp^2-type, but is intermediate between the two. The density lobes outside O(1) and O(3) are seen to be more concentrated, but not as pronounced as in the structurally similar O(2) atom in the $HC_2O_4^-$ ion (Delaplane *et al.*, 1989), where the O—H distance is only 1·036 Å and the H···O distance 1·531 Å, as compared with 1·167 and 1·270 Å in $KH(HCOO)_2$.

The peak maxima of the lone-pair regions lie in the range 0·30–0·50 e Å^{-3}. This is in good agreement with earlier experimental results for formate ions, but naturally lower than in the static theoretical maps. In α-$Ca(HCOO)_2$, NaHCOO and $LiHCOO.H_2O$ (references given above), the oxygen lone-pair peaks are between 0·15 and 0·45 e Å^{-3}.

The hydrogen bond

The electron distribution in the hydrogen bond is shown in Fig. 2. The maximum peak heights in the O(3)—H(3) and O(1)···H(3) bonds are 0·30 and 0·35 e Å^{-3}, respectively, and the electron-deficient region in the middle of the bond [close to H(3)] has a minimum of −0·15 e Å^{-3}. These densities are very similar to those found in a 100 K *X—N* study of the 2·487 Å O—H···O bond in α-oxalic acid dihydrate (Stevens & Coppens, 1980). In the 91 K *X—N* study of sodium hydrogen diacetate (Stevens, Lehmann & Coppens, 1977), peaks of 0·50 e Å^{-3} were located near the midpoints of the two equivalent O—H bonds in the 2·45 Å hydrogen bond, and the minimum at the H position was approximately −0·15 e Å^{-3}. The 100 K *X—N* maps of quinolinic acid showed a well-developed trough of −0·35 e Å^{-3} at the centre of the non-symmetric 2·400 (2) Å intramolecular O···H···O bond (Takusagawa, Kvick & Koetzle, 1978; Kvick, 1988). Here, the oxygen lone-pair peaks on both sides were

0·20 e Å^{-3}. In the 120 K X–N maps of sodium hydrogen maleate trihydrate (Olovsson, Kvick & Olovsson, 1988), the electron deficiency trough in the 2·45 Å O···O intramolecular bond was −0·30 e Å^{-3}, surrounded by two positive peaks with heights in the range 0·40–0·50 e Å^{-3}.

Thus, for the short O···O hydrogen bonds (2·40–2·50 Å) in the low-temperature studies quoted above, oxygen lone-pair peak maxima lie in the range 0·20–0·50 e Å^{-3}, and the density at the centre of the bond in the range −0·15 to −0·35 e Å^{-3}. A survey of the electron density features obtained from low-temperature studies of structures containing O···O hydrogen bonds between 2·45 and 2·80 Å (Hermansson, 1987) shows the magnitudes of peaks and troughs to be essentially independent of hydrogen-bond distance.

The peak maxima and minima in the published experimental density maps thus display no clear-cut trends with respect to hydrogen-bond distance. It should be noted, however, that the electron density at the H position is found to *decrease systematically* as the hydrogen bond gets shorter (*cf.* Hermansson, 1987), *i.e.* the H position coincides more and more with the electron-deficient region. This is due to the combined action of at least two effects: (i) the direct intermolecular interaction, whereby the hydrogen-bond-accepting oxygen pushes electrons along the O–H bond of the donating molecule, and (ii) the increased electron deficiency at the H atom due to the stretching of the O–H bond (for shorter hydrogen bonds). These two effects are counteracted to some extent by the 'juxtaposition' of the difference densities 'belonging to' neighbouring molecules. This effect makes the deformation density at the H position artificially high, since the lone-pair deformation density of the hydrogen-bond acceptor (electron excess) extends into the region of the H atom (*cf.* Eisenstein & Hirshfeld, 1983). The juxtaposition effect leads to difficulties in interpreting deformation densities in terms of truly intermolecular bonding effects.

This discussion is illustrated in Fig. 3, which shows theoretical quantum mechanical *ab-initio* deformation density maps for a model complex, $(H_2O)_3$, containing two hydrogen bonds of different lengths (O···O distances 2·50 and 3·00 Å). The O–H bond distances were 0·970 Å, and the H–O–H angles 104·5° for the hydrogen-bond donor molecules, and 105·0° for the acceptor. The basis sets used were of double-zeta plus polarization quality, *viz.* (9*s*5*p*1*d*) contracted to ⟨4*s*2*p*1*d*⟩ for O, and (4*s*1*p*) contracted to ⟨2*s*1*p*⟩ for H (Dunning, 1970; Roos & Siegbahn, 1970). The total deformation density, *i.e.* the total density for the complex *minus* the superposition of spherical atomic densities, displays a pronounced asymmetry with respect to the two hydrogen bonds (Fig. 3*a*). The apparent deformation density for three superposed unperturbed water molecules, allowing *no* intermolecular interaction, is shown in Fig. 3(*b*). The similarity between Figs. 3(*a*) and 3(*b*) shows the major part of the asymmetry in Fig. 3(*a*) to be a result of this juxtaposition effect. The effect is most apparent in the electron-deficient region of the hydrogen

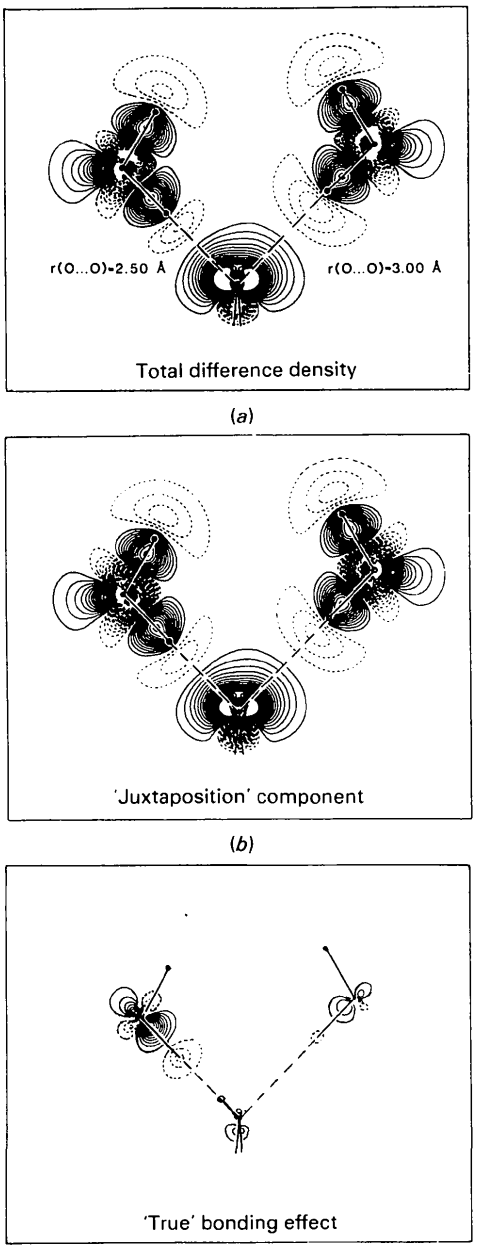

Fig. 3. Effects of intermolecular interaction and electron density juxtaposition in an $(H_2O)_3$ complex. The section displayed contains the two hydrogen-bond-donating H_2O molecules, and bisects the H–O–H angle of the hydrogen-bond-accepting molecule. Contour interval: ±0·05 e Å^{-3}. (*a*) $\rho[(H_2O)_3] - \sum\rho_{atoms}$, (*b*) $\sum_i\delta\rho[H_2O(i)]$, where $\delta\rho[H_2O(i)] = \rho[H_2O(i)] - \sum\rho_{atoms}$, (*c*) $\rho[(H_2O)_3] - \sum_i\rho[H_2O(i)]$.

bond, but even extends to the H positions. The difference between Figs. 3(*a*) and 3(*b*), *i.e.* the effect of the 'true' intermolecular interaction (Fig. 3*c*), would seem to be that the deformation density at the H position is more electron deficient for the short than for the long hydrogen bond, while juxtaposition has the opposite effect (Fig. 3*b*). The net result is a lower electron density at the H position for the shorter hydrogen bond. This would be further emphasized by O—H bond elongation which occurs in reality, but is not included in the present model calculations.

To summarize, these theoretical calculations show a variation in the electron density at the H nuclear position with respect to hydrogen-bond length. This is consistent with the low electron density found experimentally at the H position in $KH(HCOO)_2$ ($-0{\cdot}10$ e Å^{-3}), and with densities observed in other hydrogen-bonded compounds.

We would like to thank Professor Ivar Olovsson for the excellent facilities placed at our disposal. We are also indebted to Mr Hilding Karlsson for skilled technical assistance. This work has been supported by grants from the Swedish Natural Science Research Council which are gratefully acknowledged.

References

BECKER, P. & COPPENS, P. (1974). *Acta Cryst.* A**30**, 129–147.
DAM, J., HARKEMA, S. & FEIL, D. (1983). *Acta Cryst.* B**39**, 760–768.
DELAPLANE, R., TELLGREN, R. & OLOVSSON, I. (1989). *Acta Cryst.* Submitted.
DUNNING, T. H. (1970). *J. Chem. Phys.* **53**, 2823–2833.
EISENSTEIN, M. & HIRSHFELD, F. L. (1983). *Acta Cryst.* B**39**, 61–75.
FUESS, H., BATS, J. W., DANNÖHL, H., MEYER, H. & SCHWEIG, A. (1982). *Acta Cryst.* B**38**, 736–743.
FUESS, H., BURGER, N. & BATS, J. W. (1981). *Z. Kristallogr.* **156**, 219–232.
HARKEMA, S., DE WITH, G. & KEUTE, J. C. (1977). *Acta Cryst.* B**33**, 3971–3973.
HERMANSSON, K. (1987). *Acta Chem. Scand. Ser. A*, **41**, 513–526.
HERMANSSON, K., TELLGREN, R. & LEHMANN, M. S. (1983). *Acta Cryst.* C**39**, 1507–1510.
International Tables for X-ray Crystallography (1974). Vol. IV, pp. 99, 149. Birmingham: Kynoch Press. (Present distributor Kluwer Academic Publishers, Dordrecht.)
JOHANSEN, H. (1979). *Acta Cryst.* A**35**, 319–325.
KRIJN, M. P. C. M., GRAAFSMA, H. & FEIL, D. (1988). *Acta Cryst.* B**44**, 609–616.
KVICK, Å. (1988). Private communication.
LARSSON, G. & NAHRINGBAUER, I. (1968). *Acta Cryst.* B**24**, 666–672.
LEHMANN, M. S. & LARSEN, F. K. (1974). *Acta Cryst.* A**30**, 580–584.
LUNDGREN, J.-O. (1982). *Crystallographic Computer Programs.* Report UUIC-B13-04-05. Institute of Chemistry, Univ. of Uppsala, Sweden.
LUNELL, S. (1984). *J. Chem. Phys.* **80**, 6185–6193.
MCCANDLISH, L. E., STOUT, G. H. & ANDREWS, L. C. (1975). *Acta Cryst.* A**31**, 245–249.
MEULEN, J. VAN DER & FEIL, D. (1987). Private communication.
OLOVSSON, G., KVICK, Å. & OLOVSSON, I. (1988). Private communication.
ROOS, B. & SIEGBAHN, P. (1970). *Theor. Chim. Acta*, **17**, 199–208.
STEVENS, E. D. (1980). *Acta Cryst.* B**36**, 1876–1886.
STEVENS, E. D. & COPPENS, P. (1980). *Acta Cryst.* B**36**, 1864–1876.
STEVENS, E. D., LEHMANN, M. S. & COPPENS, P. (1977). *J. Am. Chem. Soc.* **99**, 2829–2831.
TAKUSAGAWA, F., KVICK, Å. & KOETZLE, T. (1978). *Acta Cryst.* A**34**, S-30.
TAURIAN, O. E., LUNELL, S. & TELLGREN, R. (1987). *J. Chem. Phys.* **86**, 5053–5059.
THOMAS, J. O. (1978). *Acta Cryst.* A**34**, 819–823.
THOMAS, J. O., TELLGREN, R. & ALMLÖF, J. (1975). *Acta Cryst.* B**31**, 1946–1955.

Acta Cryst. (1989). B**45**, 257–261

Synthesis and Structures of Tetrahedral Tetrahydrothiophene–Boron Trihalide Adducts, $C_4H_8S.BX_3$ (X = Cl, Br, I)

BY BERNT KREBS,* GERALD SCHWETLIK AND MARTIN WIENKENHÖVER

Anorganisch-Chemisches Institut der Universität Münster, Wilhelm-Klemm-Strasse 8, D-4400 Münster, Federal Republic of Germany

(*Received* 6 *August* 1988; *accepted* 3 *January* 1989)

Abstract

Tetrahydrothiophene–boron trichloride, $C_4H_8S.BCl_3$ (I), $M_r = 205{\cdot}3$, orthorhombic, $P2_12_12_1$, $a = 10{\cdot}914$ (4), $b = 9{\cdot}648$ (3), $c = 8{\cdot}165$ (3) Å, $V = 859{\cdot}8$ (5) Å^3, $Z = 4$, $D_x = 1{\cdot}59$ Mg m^{-3}, λ(Mo $K\alpha$) = 0·71069 Å, μ(Mo $K\alpha$) = 1·20 mm^{-1}, $F(000) = 433$, $T = 140$ K, $R = 0{\cdot}024$, $wR = 0{\cdot}030$ for 1076 unique observed reflections [$F > 3{\cdot}92\sigma(F)$]. Tetrahydrothiophene–boron tribromide, $C_4H_8S.BBr_3$ (II), $M_r = 338{\cdot}7$, orthorhombic, *Pnma*, $a = 10{\cdot}696$ (3), $b = 10{\cdot}182$ (2), $c = 8{\cdot}695$ (2) Å, $V = 946{\cdot}9$ (4) Å^3, $Z = 4$, $D_x = 2{\cdot}38$ Mg m^{-3}, λ(Mo $K\alpha$) = 0·71069 Å, μ(Mo $K\alpha$) = 13·66 mm^{-1}, $F(000) = 438$, $T = 140$ K, $R = 0{\cdot}044$,

* To whom correspondence should be addressed.

0108-7681/89/030257-05$03.00

© 1989 International Union of Crystallography